CAMES, **28**(2): 81–104, 2021, doi: 10.24423/cames.327

Effect of Thermal Radiation on Biomagnetic Fluid Flow and Heat Transfer over an Unsteady Stretching Sheet

Md. Jahangir ALAM[1)], Md. Ghulam MURTAZA[1)], Efstratios E. TZIRTZILAKIS[2)], Mohammad FERDOWS[3)*]

[1)] *Department of Mathematics*
Comilla University
Cumilla, Bangladesh

[2)] *Department of Mechanical Engineering*
University of the Peloponnese
Trípoli, Greece

[3)] *Research Group of Fluid Flow Modeling and Simulation*
Department of Applied Mathematics
University of Dhaka
Dhaka, Bangladesh
*Corresponding Author e-mail: ferdows@du.ac.bd

This study examines the influence of thermal radiation on biomagnetic fluid, namely blood that passes through a two-dimensional stretching sheet in the presence of magnetic dipole. This analysis is conducted to observe the behavior of blood flow for an unsteady case, which will help in developing new solutions to treat diseases and disorders related to human body. Our model is namely biomagnetic fluid dynamics (BFD), which is consistent with two principles: ferrohydrodynamic (FHD) and magnetohydrodynamic (MHD), where blood is treated as electrically conductive. It is assumed that the implemented magnetic field is sufficiently strong to saturate the ferrofluid, and the variation of magnetization with temperature may be approximated with the aid of a function of temperature distinction. The governing partial differential equations (PDEs) converted into ordinary differential equations (ODEs) using similarity transformation and numerical results are thus obtained by using the bvp4c function technique in MATLAB software with considering applicable boundary conditions. With the help of graphs, we discuss the impact of various parameters, namely radiation parameter, unsteady parameter, permeability parameter, suction parameter, magnetic field parameter, ferromagnetic parameter, Prandtl number, velocity and thermal slip parameter on fluid (blood) flow and heat transfer in the boundary layer. The rate of heat transfer and skin friction coefficient is also computationally obtained for the requirement of this study. The fluid velocity decreases with increasing values of the magnetic parameter, ferromagnetic interaction parameter, radiation parameter whereas temperature profile increases for the unsteady parameter, Prandtl number, and perme-

ability parameter. From the analysis, it is also observed that the skin friction coefficient decreases and the rate of heat transfer increases respectively with increasing values of the ferromagnetic interaction parameter. The most important part of the present analysis is that we neither neglect the magnetization nor electrical conductivity of the blood throughout this study. To make the results more feasible, they are compared with the data previously published in the literature and found to be in good accuracy.

Keywords: biomagnetic fluid, magnetohydrodynamic, ferrohydrodynamic, magnetic dipole, thermal radiation, stretching sheet.

Notation

a, b, c – constants,
x – horizontal coordinate [m],
y – vertical coordinate [m],
u – horizontal velocity [m/s],
v – vertical velocity [m/s],
t – time [s],
T – fluid temperature inside boundary layer [K],
T_w – temperature of the sheet [K],
T_∞ – fluid temperature far away from the sheet [K],
M_1 – magnetization [A/m],
H – magnetic field of intensity [A/m],
N – velocity slip factor,
K – thermal slip factor,
C_p – specific heat at constant pressure [J/(kg · K)],
U_w – stretching velocity,
V_w – suction/injection velocity,
Nu – local Nusselt number,
C_f – skin friction coefficient,
q_w – wall heat flux,
q_r – radiative heat flux,
Re – local Reynolds number,
$B(t)$ – time-dependent magnetic field intensity,
$k_1(t)$ – time-dependent magnetic permeability,
k_2 – constant permeability of the medium,
k_3 – non-dimensional permeability parameter,
k^* – mean absorption coefficient,
d – distance between magnetic dipole to sheet,
A – unsteady parameter,
Pr – Prandtl number,
M – magnetic field parameter,
S – suction parameter,
Nr – radiation parameter,
S_f – velocity y-slip parameter,
S_t – thermal l-slip parameter,
f' – dimensionless velocity components along x direction,
$f''(0)$ – skin friction.

Greek symbols:

η – similarity variable,
θ – dimensionless temperature,
$\theta'(0)$ – wall heat transfer gradient,
ψ – stream function [m^2/s],
ρ – density of the fluid [kg/m^3],
μ – dynamic viscosity [kg/ms],
ϑ – kinematic viscosity [m^2/s],
μ_0 – magnetic permeability [$kg \cdot m/A^2s^2$],
σ – electrical conductivity of the fluid [S/m],
κ – thermal conductivity [$J/m \cdot s \cdot K$],
σ^* – Stefan–Boltzman constant,
λ – viscous dissipation parameter,
ε – dimensionless Curie temperature,
β – ferromagnetic interaction parameter,
α – dimensionless distance,
τ_w – wall shear stress.

List of abbreviations:

BFD – biomagnetic fluid dynamic,
FHD – ferrohydrodynamic,
MHD – magnetohydrodynamic,
PDE – partial differential equation,
ODE – ordinary differential equation.

1. Introduction

Biological fluids (who are also a part of BFD) exist in living creatures within the presence of magnetic field generated from the action of a magnetic dipole. The most prominent biomagnetic fluid is blood. It behaves as a magnetic fluid because of the sophisticated interaction of the inter-cellular protein, cell membrane and hemoglobin that is a structure of iron oxides. In recent years, the study of BFD has attracted considerable attention from theoretical as well as experimental researchers because of its increasing usefulness and practical relevance in biomedical engineering and medical sciences, which include magnetic devices for cell separation, decreasing bleeding during surgeries, targeted transport of drugs using magnetic particles to trigger drug release,treatment of most cancer tumors causing magnetic hyperthermia, and magnetic resonance imaging (MRI) of specific parts of the human body [1–5].

Haik *et al.* [1] developed a biomagnetic fluid model based on the principle of FHD. Their study was additionally extended by another author in [6] by adopting principles of MHD and FHD and applying the developed model to investigate the flow of blood under the influence of a magnetic field. In that study,

the author stated that the blood flow may be reduced up to 40% under a strong magnetic field effect. Within the influence of magnetic dipole, a biomagnetic mathematical model through a stretching sheet was studied in [7]. The incompressible three-dimensional biomagnetic fluid that is electrically nonconducting was studied numerically in [8]. The authors assumed that the fluid magnetization varies with temperature and magnetic field strength. The significance of FHD and MHD was studied and both principles were adopted to examine biomagnetic blood flow model in [9]. The authors concluded that FHD and MHD (interaction parameters) both make significant impact on the flow field. Dual solutions on biomagnetic flow model that passes through a nonlinear stretching/shrinking sheet were presented in [10]. The flow of biomagnetic fluid with viscoelastic property over stretching sheet was studied numerically in [11]. The study of biomagnetic fluid flow and heat transfer over a stretching sheet was conducted by several researchers [12–16] with different conditions in presence of external magnetic field.

Ali *et al.* [17] examined the analytical solution of MHD blood flow through parallel plates when the lower plate exponentially expands. The impact of the magnetic dipole on ferrofluid over a stretched surface, taking into account the thermal radiation, was analyzed in [18]. Blood considered as electrical conductive phenomena under the influence of magnetic field was investigated in [19]. The unsteady blood flow over a permeable stretching sheet was investigated numerically in [20, 21] in the presence of a non-uniform heat source and sink. The impact of radiation and viscous dissipation on unsteady MHD free convective flow was analyzed in [22]. Convective flow over a porous stretch surface in the porous medium, in the presence of a heat source or sink, was studied in [23]. Thermal radiation impact on boundary layer flow under different flow conditions has been reported by several investigators in [24–28]. Newtonian fluid with the slip condition taken into consideration was studied in [29]. In [30], fluid flow and heat transfer on a stretched sheet were studied and variable viscosity with slip conditions was considered.

Moreover, an incompressible electrified Maxwell ferromagnetic liquid flow through a two-dimensional stretching sheet in the presence of a rotating magnetic field along with heat generation/absorption was investigated in [31]. The authors found that velocity and temperature profile decreases and increases with increasing values of the ferromagnetic parameter, respectively. The behavior of ferrofluid over a cylindrical rotating disk with temperature-dependent viscosity was investigated in [32]. The flow and heat transfer of ferrofluid over a permeable stretching sheet with the effects of suction/injection have been examined in [33]. The viscoelastic property of the fluid in MHD flow and heat transfer over a two-dimensional stretching sheet under slip velocity was studied in [34]. The flow and convective heat transfer analysis of dusty ferrofluid over a stretching

surface have been presented in [35]. The authors noted that temperature profile increases with enhanced values of the ferromagnetic parameter in both the ferrofluid phase and dusty phase. It is also clear from that study that the ferrofluid phase is significantly more comprising than a dusty phase. The effects of thermal radiation on the ferrofluid flow and heat transfer over a stretching sheet were discussed in [36].

The goal of the present analysis is to investigate the BFD flow and heat transfer of blood along a stretched sheet under the influence of thermal radiation. For the mathematical formulation, we adopt the version of BFD consistent with FHD and MHD principles. A similarity transformation is used to convert the nonlinear PDEs into nonlinear ODEs. The effects of various relevant parameters on the momentum and heat transfer have been investigated and the numerical results are presented graphically and in tabular form. The aim is that the present study will be used in the biotechnology and medical sciences.

2. Model descriptions

Consider an unsteady, two-dimensional boundary layer flow of an incompressible electrically conducting biomagnetic fluid, namely blood passing through a stretched sheet with velocity $U_w(x,t) = \frac{ax}{1-ct}$, where a and c are constant such that $a > 0$, $c \geq 0$ and $ct < 1$ (Fig. 1). X – axes are taken along the sheet and Y – axes are chosen normal to it. It is assumed that the sheet is kept at constant temperature T_w, and T_∞ is the temperature of the ambient fluid where

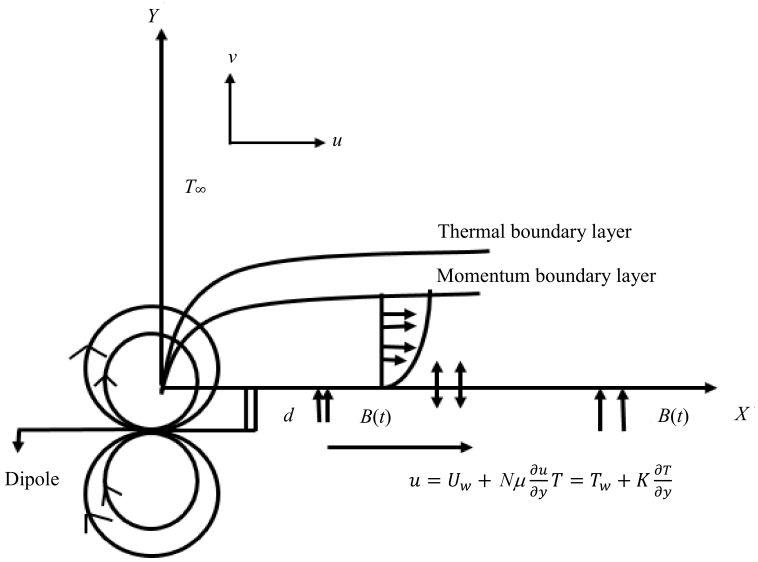

Fig. 1. Schematic diagram of the flow problem.

$T_w < T_\infty$. A transverse magnetic field of strength $B(t) = \frac{B_0}{(1-ct)^{1/2}}$ is applied in the Y – direction and at $t = 0$, B_0 corresponds to the constant magnetic field strength. A magnetic dipole generates a magnetic field of strength H, which is supposed to be located some distance d from the sheet. Under these assumptions, continuity, momentum and energy equations are taken in the following form [12].

Continuity equation:

$$\frac{\partial u}{\partial x} + \frac{\partial v}{\partial y} = 0. \tag{1}$$

Momentum equation:

$$\frac{\partial u}{\partial t} + u\frac{\partial u}{\partial x} + v\frac{\partial u}{\partial y} = \vartheta\frac{\partial^2 u}{\partial y^2} - \frac{\sigma B^2(t)}{\rho}u - \frac{\vartheta}{k_1\,(t)}u + \frac{\mu_0}{\rho}M_1\frac{\partial H}{\partial x}. \tag{2}$$

Energy (Heat) equation:

$$\rho C_p\left(\frac{\partial T}{\partial t} + u\frac{\partial T}{\partial x} + v\frac{\partial T}{\partial y}\right) + \mu_0 T\frac{\partial M_1}{\partial T}\left(u\frac{\partial H}{\partial x} + v\frac{\partial H}{\partial y}\right) = \kappa\frac{\partial^2 T}{\partial y^2} - \frac{\partial q_r}{\partial y}, \tag{3}$$

where u and v represents the velocity component along x- and y-direction, ρ and $B(t)$ represents the biomagnetic fluid density and time-dependent magnetic field intensity, respectively, $k_1(t) = k_2(1 - ct)$ is the time-dependent permeability parameter, k_2 is initial permeability, κ and C_p denotes the thermal conductivity and specific heat, respectively, ϑ is the kinematic coefficient, σ is electrical conductivity, q_r implies radiative heat flux, M indicates magnetization, H is magnetic field of strength, T is the temperature of field, and μ_0 is magnetic permeability.

The associated boundary conditions for the given mathematical problem are in the following form [37, 38]:

$$\begin{aligned} &y = 0 : u = U_w + N\mu\frac{\partial u}{\partial y}, \quad v = V_w, \quad T = T_w + K\frac{\partial T}{\partial y}, \\ &y \to \infty : u \to 0, \quad T \to T_\infty, \end{aligned} \tag{4}$$

where V_w specifies the injection/suction velocity and it is in the following form:

$$V_w = -\sqrt{\frac{\vartheta U_w}{x}}f(0). \tag{5}$$

Equation (5) expresses that mass transfer occurs with velocity V_w from the surface of the wall, where $V_w > 0$ and $V_w < 0$ describe injection and suction, respectively. In Eq. (4), $N = N_0(1 - ct)^{1/2}$ and $K = K_0(1 - ct)^{1/2}$ are velocity

and thermal slip factor, respectively. The no-slip conditions can be recovered instead of putting $N = K = 0$. The temperature of the stretched sheet $T_w(x,t)$ is assumed in the following form:

$$T_w(x,t) = T_\infty + \frac{bx}{1-ct}, \tag{6}$$

where b and c are positive constants such that $b,\ c \geq 0$ having a dimension "$time^{-1}$" and $ct < 1$.

The radiation heat flux q_r is simulated according to the Rossel and approximation [39] such that

$$q_r = \frac{4\sigma^*}{3k^*}\frac{\partial T^4}{\partial y}, \tag{7}$$

where σ^* and k^* are the Stefan–Boltzman constant and the mean absorption coefficient. Following [39], we assumed that the temperature differences within the flow are such that the term T^4 may be expressed as a linear function of the temperature, we expand T^4 in a Taylor series about T_∞ and neglecting the higher-order terms beyond the first degree in $(T - T_\infty)$ we get

$$T^4 \cong 4TT_\infty^3 - 3T_\infty^4. \tag{8}$$

Employing Eqs (7) and (8) in (3), the energy equation reduces to

$$\rho C_p\left(\frac{\partial T}{\partial t} + u\frac{\partial T}{\partial x} + v\frac{\partial T}{\partial y}\right) + \mu_0 T\frac{\partial M_1}{\partial T}\left(u\frac{\partial H}{\partial x} + v\frac{\partial H}{\partial y}\right) = \kappa\frac{\partial^2 T}{\partial y^2} + \frac{16\ \sigma^*\ T_\infty^3}{3k^*}\frac{\partial^2 T}{\partial y^2}. \tag{9}$$

The partial part of $\frac{\mu_0}{\rho}M_1\frac{\partial H}{\partial x}$ in Eq. (2) denotes the ferromagnetic body force per unit volume, while the term $\mu_0 T\frac{\partial M_1}{\partial T}\left(u\frac{\partial H}{\partial x} + v\frac{\partial H}{\partial y}\right)$ in Eq. (3) indicates heating due to adiabatic magnetization. According to the [40], we assumed that the component H_x and H_y of the magnetic field $\mathbf{H} = (H_x, H_y)$ due to a magnetic dipole that is located at a distance d below the sheet can be written in the following form:

$$H_x(x,y) = -\frac{\partial V}{\partial x} = \frac{\gamma}{2\pi}\frac{x^2 - (y+d)^2}{[x^2 + (y+d)^2]^2}, \tag{10}$$

$$H_y(x,y) = -\frac{\partial V}{\partial y} = \frac{\gamma}{2\pi}\frac{2x(y+d)}{[x^2 + (y+d)^2]^2}, \tag{11}$$

where

$$V = \frac{\alpha}{2\pi}\frac{x}{x^2 + (y+d)^2}$$

depict the magnetic scalar potential in the region of a magnetic dipole, $\gamma = \alpha$ and α is a dimensionless distance defined as

$$\alpha = \sqrt{\frac{U_w}{\vartheta x}}d.$$

Due to the magnetic body forces corresponding to the gradients of magnitude $\|\mathbf{H}\| = H$, we obtain

$$H(x,y) = \left[H_x^2 + H_y^2\right]^{1/2} = \frac{\gamma}{2\pi}\left[\frac{1}{(y+d)^2} - \frac{x^2}{(y+d)^4}\right]. \tag{12}$$

Thus the corresponding horizontal and vertical components of the magnetic field are expressed in the form

$$\begin{cases} \dfrac{\partial H}{\partial x} = \dfrac{\gamma}{2\pi}\dfrac{-2x}{(y+d)^4}, \\ \dfrac{\partial H}{\partial y} = \dfrac{\gamma}{2\pi}\left[\dfrac{-2}{(y+d)^3} + \dfrac{4x^2}{(y+d)^5}\right]. \end{cases} \tag{13}$$

Following [41], we assume that the impact of magnetization M varies with temperature T defined by the expression in the following form:

$$M_1 = K(T - T_\infty), \tag{14}$$

where K is a pyromagnetic coefficient.

3. Transformation to non-dimensionalize

Equations (2) and (9) are made dimensionless with considering the following transformation [12]:

$$\eta = \sqrt{\frac{U_w}{\vartheta x}}y, \qquad \psi = \sqrt{\vartheta x U_w}f(\eta), \qquad \theta(\eta) = \frac{T - T_\infty}{T_w - T_\infty}, \tag{15}$$

where ψ, $\theta(\eta)$ and η are a stream function, dimensionless temperature function, and dimensionless similarity variable, respectively.

Continuity Eq. (1) is satisfied automatically by expressing the stream function in the following form:

$$u = \frac{\partial \psi}{\partial y} \qquad \text{and} \qquad v = -\frac{\partial \psi}{\partial x}.$$

Using Eqs (10) to (15), we convert (2) and (7) into a set of following ODEs and boundary conditions:

$$f''' - f'^2 + ff'' - A\left[f' + \frac{1}{2}\eta\, f''\right] - M^2 f' - \frac{1}{k_3}f' - \frac{2\beta\theta}{(\eta+\alpha)^4} = 0, \tag{16}$$

$$\frac{(1+Nr)}{\Pr}\theta'' - A\left(\theta + \frac{1}{2}\eta\theta'\right) - f'\theta + f\theta' - 2\beta\lambda\frac{(\varepsilon+\theta)}{\Pr(\eta+\alpha)^3}f = 0, \tag{17}$$

$$\eta = 0 : f = S, \qquad f' = 1 + S_f f'', \qquad \theta = 1 + S_t\theta'', \tag{18}$$

$$\eta \to \infty : f' \to \theta \to . \tag{19}$$

In Eq. (18), S symbolizes suction and injection parameter if $S > 0$ and if $S < 0$ respectively, which is used to control the strength of direction of flow at the boundary. In equations written above, primes denote derivatives with respect to η.

Here the parameters that appears in Eqs (16)–(19) are expressed and defined as:

$\Pr = \dfrac{\mu C_p}{\kappa}$ – Prandtl number,

$A = \dfrac{c}{a}$ – unsteady parameter,

$k_3 = \dfrac{ak_2}{\vartheta}$ – permeability parameter,

$Nr = \dfrac{16\sigma^* T_\infty^3}{3\kappa k^*}$ – radiation parameter,

$\lambda = \dfrac{a\mu^2}{\rho k(1-ct)(T_w - T_\infty)}$ – viscous dissipation parameter,

$\beta = \dfrac{\gamma}{2\pi}\dfrac{\mu_0 K(T_w - T_\infty)\rho}{\mu^2}$ – ferromagnetic interaction parameter,

$M = B_0\sqrt{\dfrac{\sigma}{\rho a}}$ – magnetic field parameter,

$\varepsilon = \dfrac{T_\infty}{T_w - T_\infty}$ – dimensionless Curie temperature,

$\alpha = \sqrt{\dfrac{U_w}{\vartheta x}}d$ – dimensionless distance,

$S_f = N_0\rho\sqrt{a\vartheta}$ – velocity-slip parameter,

$S_t = K_0\sqrt{\dfrac{a}{\vartheta}}$ – thermal-slip parameter.

The skin friction and local Nusselt number are interesting physical quantities which mathematically are defined as:

$$C_f = \frac{2\tau_w}{\rho U_w^2} \qquad \text{and} \qquad \mathrm{Nu} = \frac{x q_w}{\kappa(T_w - T_\infty)}.$$

The wall shear stress τ_w and the heat flux q_w are determined in the following way:

$$\tau_w = \mu \left(\frac{\partial u}{\partial y}\right)_{y=0} \qquad \text{and} \qquad q_w = -\kappa \left(\frac{\partial T}{\partial y}\right)_{y=0}.$$

Finally, the skin friction coefficient and Nusselt number are made dimensionless and take the following form:

$$C_f = 2\mathrm{Re}^{-1/2} f''(0), \qquad \mathrm{Nu} = -\mathrm{Re}^{1/2}\theta'(0),$$

where the local Reynolds number is defined as

$$\mathrm{Re} = \frac{x U_w}{\vartheta}.$$

4. Numerical method

In this section, we discuss the numerical method of the studied problem given in (16) and (17) subject to the boundary conditions (18) and (19) that are built in MATLAB software by using the bvp4c function technique. For this purpose, we convert the boundary conditions and the higher-order PDEs into a set of first-order differential equations by considering new variables. Let us define some new variables as: $f = y_1$, $f' = y_2$, $f'' = y_3$, $\theta = y_4$, $\theta' = y_5$.

Then the system of first-order differential equations is given as follows:

$$\begin{cases} f' = y_2, \\ f'' = y_2' = y_3, \\ f''' = y_3' = A(y_2 + \dfrac{\eta}{2} y_3) + y_2^2 - y_1 y_3 + \dfrac{2\beta y_4}{(\eta+\alpha)^4} + M^2 y_2 + \frac{y_2}{\kappa_3}, \\ \theta' = y_5, \\ \theta'' = y_5' = \dfrac{\mathrm{Pr}}{(1+Nr)} \left\{ A\left(y_4 + \dfrac{\eta}{2} y_5\right) + y_2 y_4 - y_1 y_5 \right\} + \dfrac{1}{(1+Nr)} \dfrac{2\beta\lambda y_1(\varepsilon + y_4)}{(\eta+\alpha)^3}, \end{cases} \tag{20}$$

and the initial boundary conditions:

$$\begin{aligned} &y_1(0) = S, \qquad y_2(0) = 1 + S_f y_3(0), \qquad y_4(0) = 1 + S_t y_5(0), \\ &y_2(\infty) = 0, \qquad y_4(\infty) = 0. \end{aligned} \tag{21}$$

The initial boundary conditions (21) and Eq. (20) are integrated numerically as an initial value problem to a given terminal point. All these simplifications have been done using the MATLAB package.

5. Parameter estimated

In this work, we examine the influence of radiation on the blood flow that passes through the stretched sheet. To obtain the numerical answer, it is necessary to determine some unique values for the dimensionless parameters such as unsteadiness parameters, suction parameters, permeability parameters, velocity slip parameters, thermal slip parameter, Prandtl number, radiation parameter, magnetic field parameter, and ferromagnetic parameter, which all make a significant impact on the biomagnetic flow. Many scientists have been documented in the scientific literature using different values of dimensionless parameters in handling the flow problem. We assume that the fluid is blood, and take the following values into account:

$$\mu = 3.2 \times 10^{-3} \text{ kg/m} \cdot \text{s}, \qquad \rho = 1050 \text{ kg/m}^3, \tag{22}$$

$$C_p = 14.65 \text{ J/kg} \cdot \text{K}, \quad \kappa = 2.2 \times 10^{-3} \text{ J/m} \cdot \text{s} \cdot \text{K}. \tag{23}$$

Using these values, we have $\Pr = \frac{\mu C_p}{\kappa} = 21$.

We assume that the human body temperature is $T_w = 37°\text{C}$ [43] and the body Curie temperature is $T_\infty = 41°\text{C}$, hence the dimensionless temperature is $\varepsilon = 78.5°\text{C}$.

We use the value of the following parameters in Figs 2–27.

The ferromagnetic interaction parameter $\beta = 0$ to 10 as in [9, 10]. Note that $\beta = 0$ corresponds to the hydrodynamatic flow, unsteadiness parameter $A = 0$, 0.5, 1 as in [12], permeability parameter $k_3 = 0.2$, 0.3, 0.4, 1 as in [12], radiation parameter $Nr = 1$, 2, 3 as in [12], Prandtl number $\Pr = 21$, 23, 25 as in [10, 12], values of dimensionless distance $\alpha = 1$ as in [7], magnetic field parameter $M = 1$, 2, 3 as in [9, 12], velocity slip parameter $S_f = 1$, 1.5, 2.5 as in [12], thermal slip parameter $S_t = 0.5$, 1, 1.5 as in [12], viscous dissipation parameter $\lambda = 1.6 \times 10^{-14}$, and suction parameter $S = 0.5$, 1, 1.5 as in [12].

6. Results and discussion

We compare the values of the local Nusselt number $-\theta'(0)$ with the work presented in [44–47] to determine the validity of the numerical analysis by way of replacing $S = 0$, $S_f = 0$, $S_t = 0$, $\beta = 0$, $\lambda = 0$, $A = 0$, $k_3 \to \infty$. The comparison shown in Table 1 suggests a very good agreement.

TABLE 1. Comparison of Nusselt number $-\theta'(0)$ for different values Nr, M, Pr.

Nr	M	Pr	Magyari and Keller [44]	El-Aziz [45]	Bidin and Nazar [46]	Ishak [47]	Present results
0	0	1	−0.954782	−0.954785	−0.9548	−0.9548	−0.95481
–	–	2	–	–	−1.4714	−1.4715	−1.471443
–	–	3	−1.869075	−1.869074	−1.8691	−1.8691	−1.869059
–	–	5	−2.500135	−2.500132	–	−2.5001	−2.500119
–	–	10	−3.660379	−3.660372	–	−3.6604	−3.660360
–	1	1	–	–	–	−0.8611	−0.861221
1	0	–	–	–	−0.5315	−0.5312	−0.531158
1	–	–	–	–	–	−0.4505	−0.450536

The effect of the magnetic field parameters on the distributions of velocity and temperature can be found in Figs 2 and 3, respectively. We see that the fluid

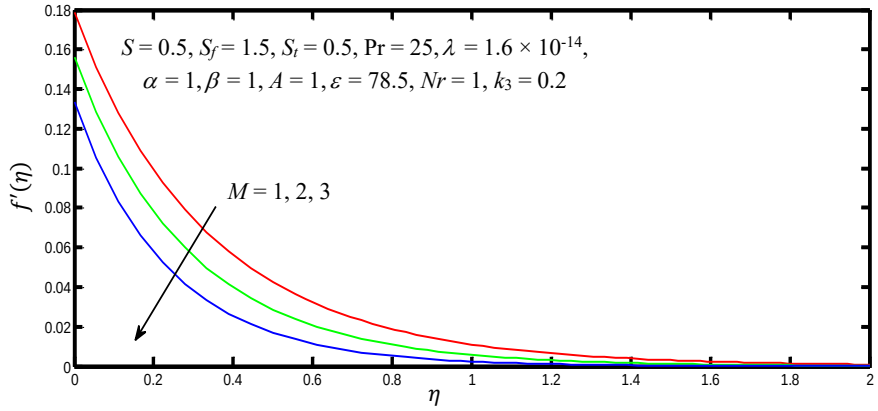

FIG. 2. The behavior of $f'(\eta)$ against M.

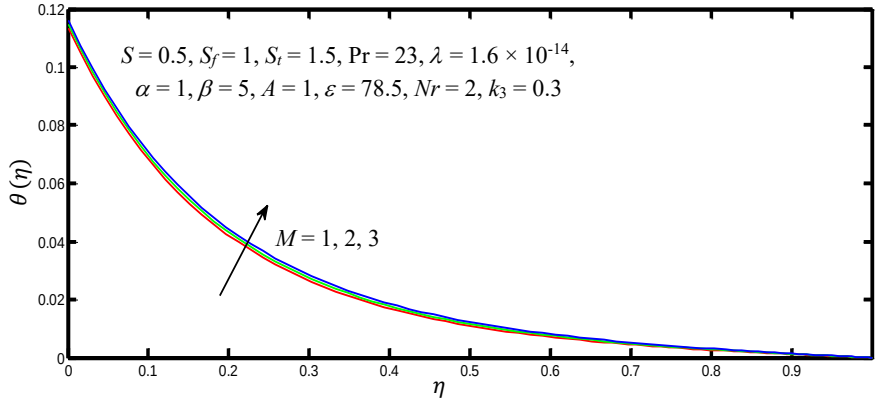

FIG. 3. The behavior of $\theta(\eta)$ against M.

velocity decreased with an improvement in the magnetic field parameter, and the boundary layer temperature increased with the same improvement. This shows specifically that the transverse magnetic field opposes transport phenomena. We see that the fluid velocity decreased with an improvement in the magnetic field parameter, and the boundary layer temperature increased in the same case. Consequently, there is a tendency for the transverse magnetic field to create a drag force called the Lorentz force.

The influence of radiation parameter on velocity and temperature profiles is illustrated in Figs 4 and 5. Figures 4 and 5 demonstrate that fluid velocity decreases with rising values of radiation parameter while in this case temperature profile enhanced. Temperature profiles increase because the conduction impact of the fluid increases in the presence of radiation.

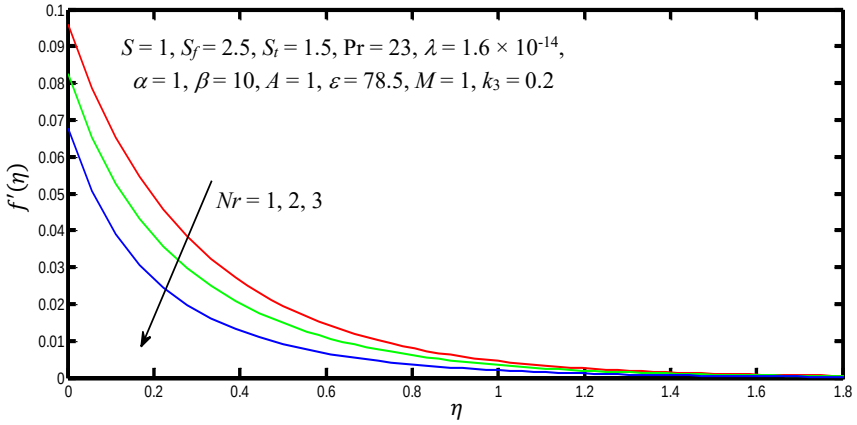

FIG. 4. The behavior of $f'(\eta)$ against Nr.

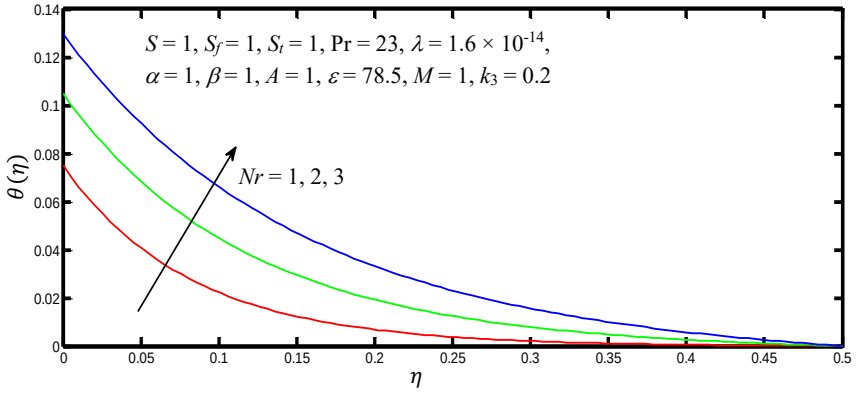

FIG. 5. The behavior of $\theta(\eta)$ against Nr.

Figures 6 and 7, respectively, depict the effect of the Prandtl number (Pr) on velocity and temperature distributions. Figure 6 demonstrates that the velocity

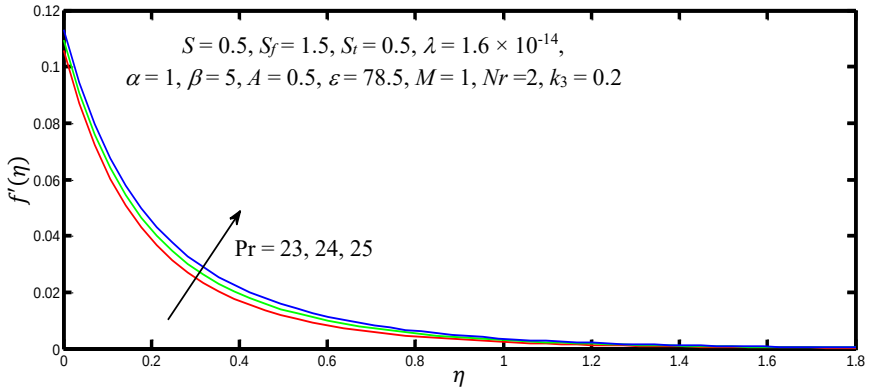

FIG. 6. The behavior of $f'(\eta)$ against Pr.

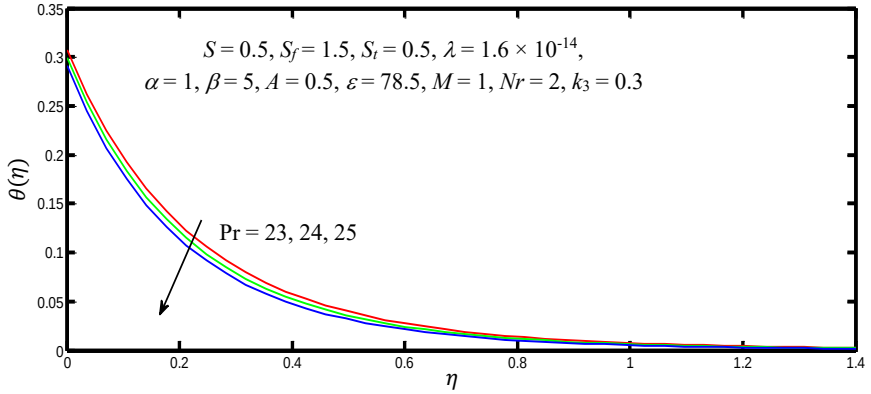

FIG. 7. The behavior of $\theta(\eta)$ against Pr.

profile increases with increasing the value of the Prandtl number and Fig. 7 shows that the temperature decreases with increasing value of the Prandtl number due to the increase of fluid heat capacity or the decrease of the thermal diffusivity. Hence, this causes a decrease of the thermal expansion influence on the flow.

The effect of unsteadiness parameters on velocity and temperature profiles is illustrated in Figs 8 and 9. In Fig. 8 it is observed that the boundary layer increases as the values of the unsteadiness parameter (A) increase. The steady case occurs for $A = 0$. Figure 9 shows that the temperature is found to decrease with an increase at a particular stage. It is also observed that the transferred heat from the sheet to the fluid also decreases with the parameter of unsteadiness increasing as a consequence of the gradual decrease in the heat transferred from the sheet to the fluid.

Figures 10 and 11 show the effect of ferromagnetic interaction parameter (β) on dimensionless velocity and temperature profiles. It can be observed in Fig. 10 that the velocity of the fluid decreases with an increase of ferromagnetic number,

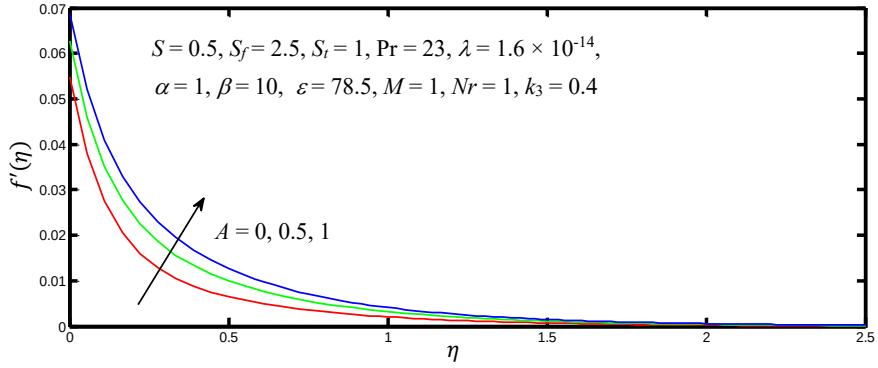

FIG. 8. The behavior of $f'(\eta)$ against A.

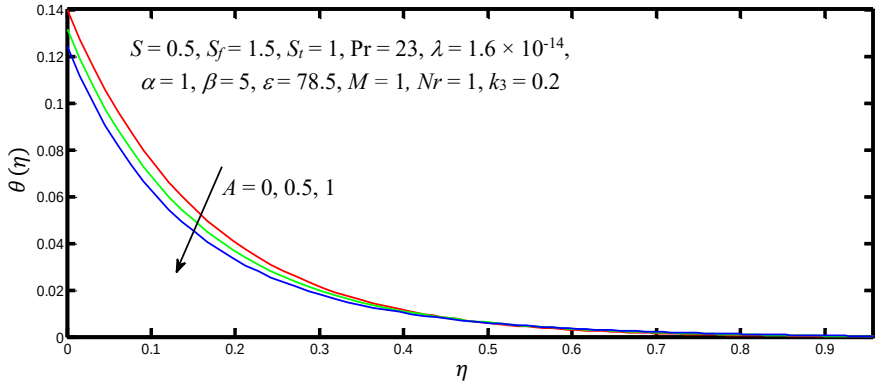

FIG. 9. The behavior of $\theta(\eta)$ against A.

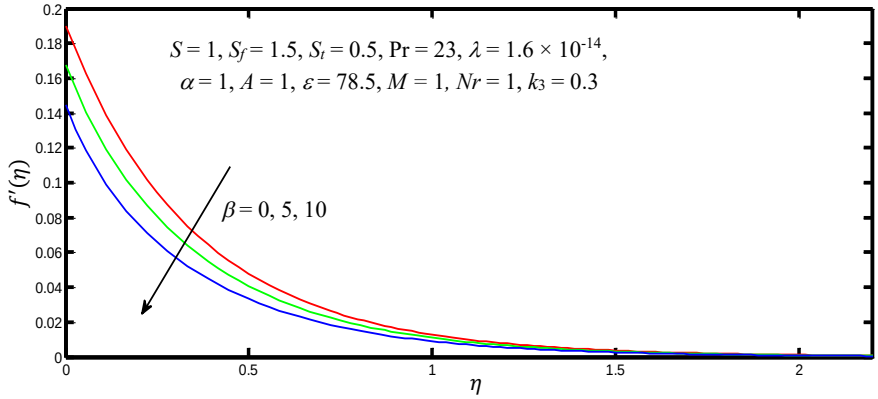

FIG. 10. The behavior of $f'(\eta)$ against β.

whereas Fig. 11 shows that the temperature profile increases in this case. This is because the ferromagnetic number is directly related to Kelvin force, which is also known as drug force and it is the same as in Figs 2 and 3.

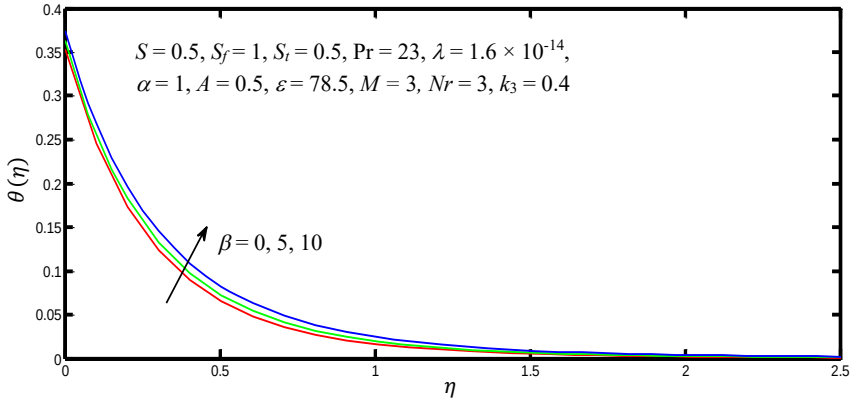

FIG. 11. The behavior of $\theta(\eta)$ against β.

Variations of velocity and temperature profiles are displayed in Figs 12 and 13 for various values of permeability parameter. It can be seen in Fig. 12 that

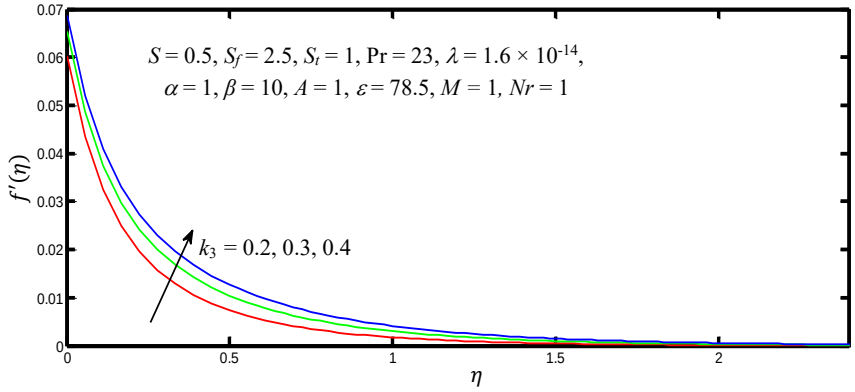

FIG. 12. The behavior of $f'(\eta)$ against k_3.

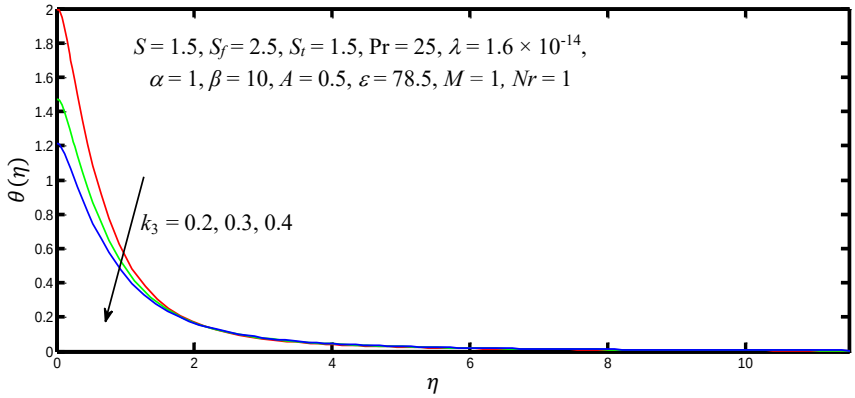

FIG. 13. The behavior of $\theta(\eta)$ against k_3.

the velocity profile increases with increasing permeability parameter (k_3). The important fact is that the fluid flow increases in the sheet as the permeability parameter (k_3) increases. The resistance of the sheet may be neglected when the hole becomes larger in the sheet. This is the reason behind that the velocity at the bottom is observed to be zero and it reaches the maximum when it reaches the free surface. Figure 13 shows that the temperature distribution decreases with increasing values of permeability parameter (k_3).

The effect of slip parameter on the distribution of velocity and temperature can be found in Figs 14 and 15, respectively. The fluid velocity profile is shown to decrease in Fig. 14 as the velocity slip factor increases. The reason behind it is that under slip conditions, the drag of the sheet is partly transmitted to the fluid. Figure 15 indicates that the temperature profile at every point in the flow sheet increases with increasing values of the velocity slip factor.

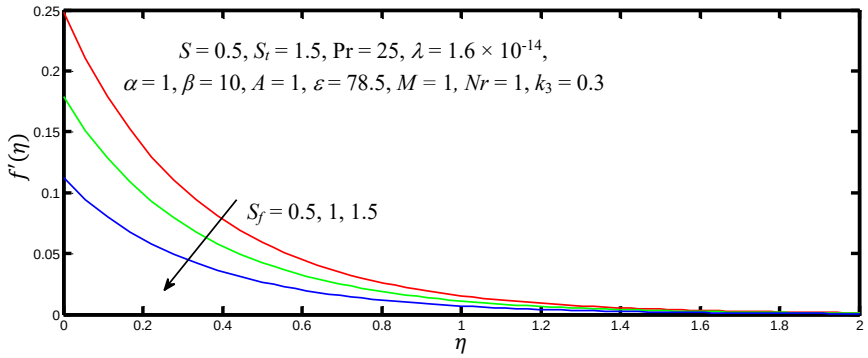

FIG. 14. The behavior of $f'(\eta)$ against S_f.

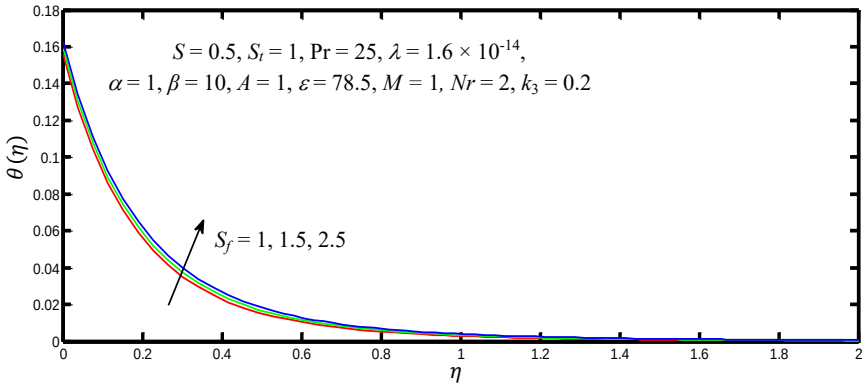

FIG. 15. The behavior of $\theta(\eta)$ against S_f.

The impact of the thermal slip parameter (S_t) on velocity and temperature profiles can be found in Figs 16 and 17. As the thermal slip factor steadily

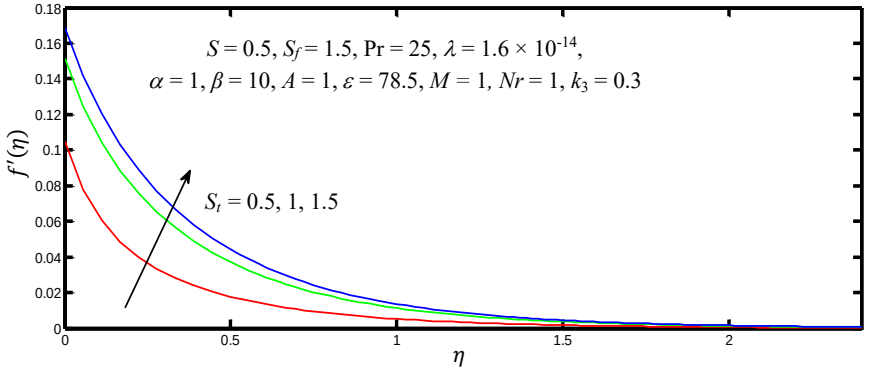

FIG. 16. The behavior of $f'(\eta)$ against S_t.

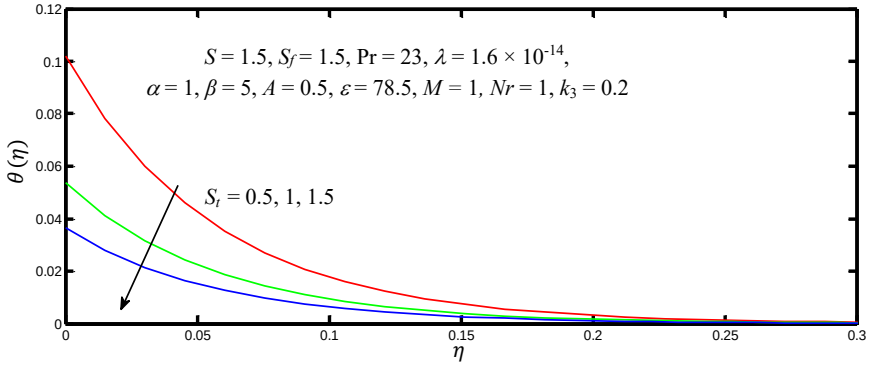

FIG. 17. The behavior of $\theta(\eta)$ against S_t.

increases, Fig. 16 shows that the velocity profile increases. In Fig. 17, it is found that temperature decreases as the thermal slip factor (S_t) increases. The heat transmitted from the stretched sheet to the fluid increases due to the thermal slip factor.

Figures 18 and 19 display the velocity and temperature profiles for various values of the suction parameter (S). With increasing values of the suction, it is seen in Fig. 18 that the velocity decreases. The reason behind that the suction moves the fluid away from the sheet surface, and as a result, the boundary layer decreases. The temperature profile in the flow region decreases with increasing values of the suction parameter (S), which is clearly seen in Fig. 19. Since the suction parameter increases, more fluid is taken away from the fluid area, thus causing thermal boundary layer thickness to decrease.

Figures 20–27 portray the influence of various parameters such as ferromagnetic number β, unsteadiness parameter A, suction parameter S, Prandtl number Pr with regard to magnetic field parameter on skin friction coefficient and rate of heat transfer. This clearly indicates that skin friction decreases with in-

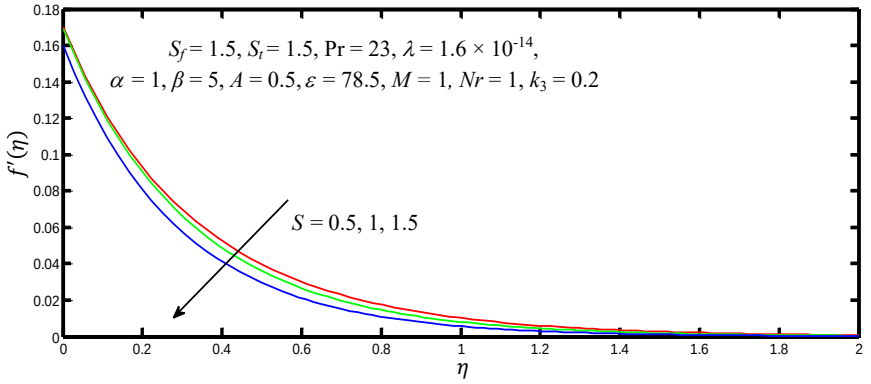

FIG. 18. The behavior of $f'(\eta)$ against S.

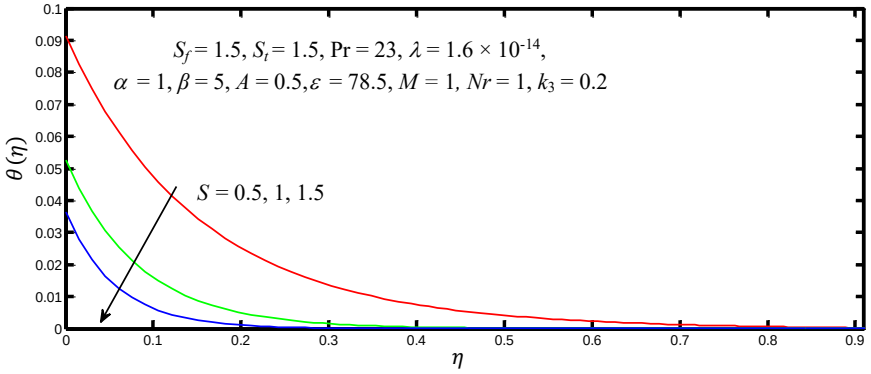

FIG. 19. The behavior of $\theta(\eta)$ against S.

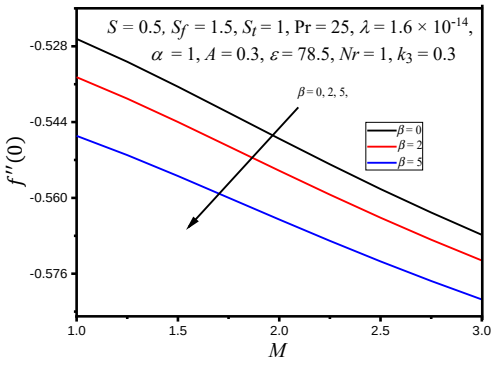

FIG. 20. $f''(0)$ against β.

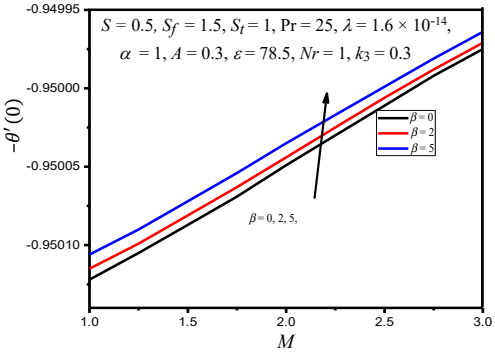

FIG. 21. $-\theta'(0)$ against β.

creasing values of the ferromagnetic number, whereas the rate of the wall heat transfer increases in this case. The skin friction is also observed to increase with increasing Prandtl number values, while, in this case, the rate of the wall heat

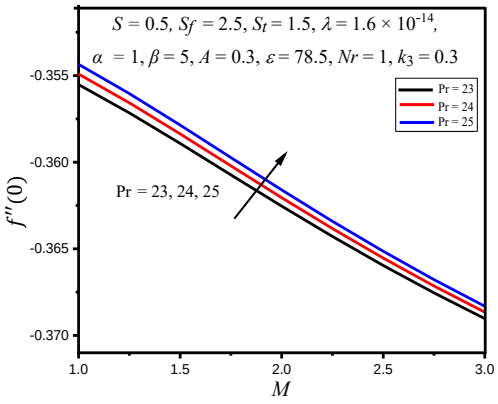

FIG. 22. $f''(0)$ against Pr.

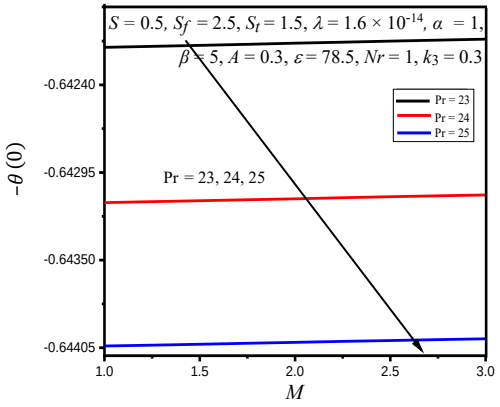

FIG. 23. $-\theta'(0)$ against Pr.

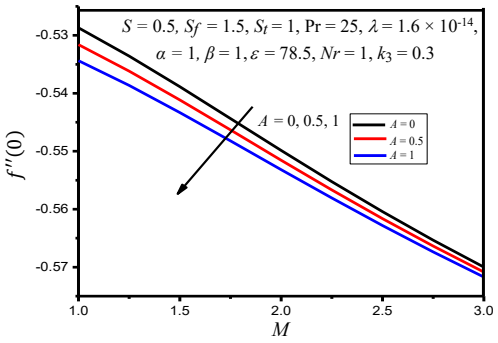

FIG. 24. $f''(0)$ against A.

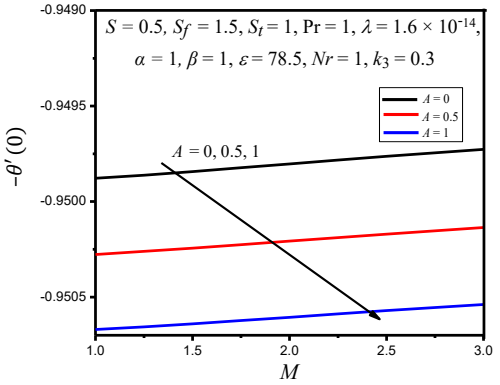

FIG. 25. $-\theta'(0)$ against A.

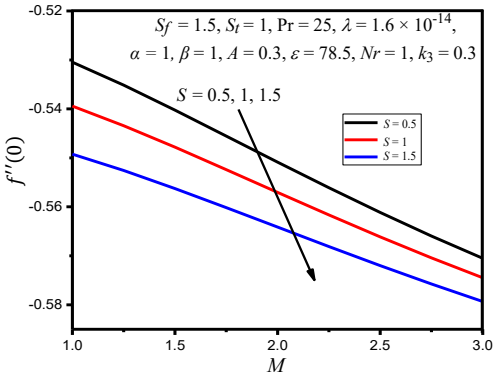

FIG. 26. $f''(0)$ against S.

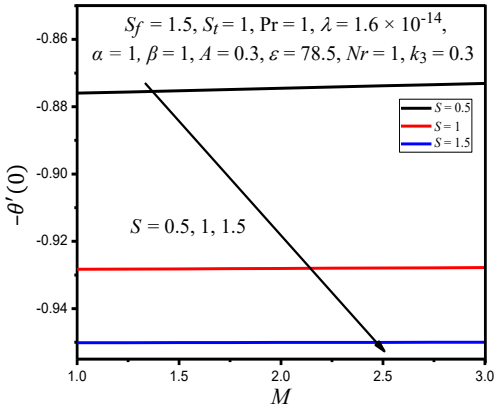

FIG. 27. $-\theta'(0)$ against S.

transfer decreases. But with the unsteadiness parameter and suction parameter increased values, both the skin friction and rate of wall heat transfer decrease.

7. Conclusion

In this article, we examined the influence of thermal radiation on the BFD flow under the applied magnetic field action. The main findings are as follows:

1) The magnetic field parameter, radiation parameter, ferromagnetic interaction parameter, and velocity slip parameter lead to alleviated/lessened the fluid velocity, whereas temperature increased in all cases.
2) The fluid velocity increased with increasing values of the Prandtl number, unsteadiness parameter, permeability parameter, and non-dimensional thermal slip factor, while the temperature decreased in all cases.
3) An increase in the suction parameter reduced both fluid velocity and temperature.
4) With increasing values of ferromagnetic interaction parameters, the skin friction decreased, while the rate of heat transfer increased.
5) The Prandtl number reduced the local Nusselt number where as the skin friction coefficient increased in this case.
6) The unsteadiness parameter and suction parameter reduced both the skin friction coefficient and rate of heat transfer.

References

1. Y. Haik, J.C. Chen, V.M. Pai, Development of biomagnetic fluid dynamics, [in:] Proceedings of the IX International Symposium on Transport Properties in Thermal Fluid Engineering, Singapore, Pacific Center of Thermal Fluid Engineering, S.H. Winoto, Y.T. Chew, N.E. Wijeysundera [Eds], Hawaii, USA, June 25–28, pp. 121–126, 1996.
2. P.A. Voltairas, D.I. Fotiadis, L.K. Michalis, Hydrodynamics of magnetic drug targeting, *Journal of Biomechanics*, **35**(6): 813–821, 2002, doi: 10.1016/S0021-9290(02)00034-9.
3. E.K. Ruuge, A.N. Rusetski, Magnetic fluid as drug carriers: Targeted transport of drugs by a magnetic field, *Journal of Magnetism and Magnetic Materials*, **122**(1–3): 335–339, 1993, doi: 10.1016/0304-8853(93)91104-F.
4. W.-L. Lin, J.-Y.Yen, Y.-Y. Chen, K.-W. Jin, M.-J. Shieh, Relationship between acoustic aperture size and tumor conditions for external ultrasound hyperthermia, *Medical Physics*, **26**(5): 818–824, 1999, doi: 10.1118/1.598590.
5. J.C. Misra, A. Sinha, G.C. Shit, Flow of a biomagnetic viscoelastic fluid: Application to estimation of blood flow in arteries during electromagnetic hyperthermia, a therapeutic procedure for cancer treatment, *Applied Mathematics and Mechanics*, **31**(11): 1405–1420, 2010, doi: 10.1007/s10483-010-1371-6.
6. E.E. Tzirtzilakis, A mathematical model for blood flow in magnetic field, *Physics of Fluids*, **17**(7): 077103-1-14, 2005, doi: 10.1063/1.1978807.
7. N.G. Kafoussias, E.E. Tzirtzilakis, Biomagnetic fluid flow over a stretching sheet with nonlinear temperature dependent magnetization, *The Journal of Applied Mathematics and Physics (ZAMP)*, **54**: 551–565, 2003, doi: 10.1007/s00033-003-1100-5.

8. E.E. Tzirtzilakis, N.G. Kafoussias, Three-dimensional magnetic fluid boundary layer flow over a linearly stretching sheet, *Journal of Heat Transfer*, **132**(1): 011702-1-8, 2010, doi: 10.1115/1.3194765.

9. M.G. Murtaza, E.E. Tzirtzilakis, M. Ferdows, Effect of electrical conductivity and magnetization on the biomagnetic fluid flow over a stretching sheet, *The Journal of Applied Mathematics and Physics (ZAMP)*, **68**: 93, 2017, doi: 10.1007/s00033-017-0839-z.

10. M. Ferdows, G. Murtaza, E.E. Tzirtzilakis, J.C. Misra, A. Alsenafi, Dual solutions in biomagnetic fluid flow and heat transfer over a nonlinear stretching/shrinking sheet: Application of Lie group transformation method, *Mathematical Biosciences and Engineering*, **17**(5): 4852–4874, 2020, doi: 10.3934/mbe.2020264.

11. J.C. Misra, G.C. Shit, Biomagnetic viscoelastic fluid flow over a stretching sheet, *Applied Mathematics and Computation*, **210**(2): 350–361, 2009, doi: 10.1016/j.amc.2008.12.088.

12. J.C. Misra, A. Sinha, Effect of thermal radiation on MHD flow of blood and heat transfer in a permeable capillary in stretching motion, *Heat and Mass Transfer*, **49**: 617–628, 2013, doi: 10.1007/s00231-012-1107-6.

13. N.G. Kafoussias, E.E. Tzirtzilakis, A. Raptis, Free forced convective boundary layer flow of a biomagnetic fluid under the action of a localized magnetic field, *Canadian Journal of Physics*, **86**(3): 447–457, 2008, doi: 10.1139/p07-166.

14. M.G. Murtaza, E.E. Tzirtzilakis, M. Ferdows, Similarity solutions of nonlinear stretched biomagnetic fluid flow and heat transfer with signum function and temperature power law geometries, *International Journal of Mathematical and Computational Sciences*, **12**(2): 24–29, 2018, doi: 10.5281/zenodo-1315703.

15. M. Murtaza, E.E. Tzirtzilakis, M. Ferdows, Stability and convergence analysis of a biomagnetic fluid flow over a stretching sheet in the presence of a magnetic dipole, *Symmetry*, **12**(2): 253, 2020, doi: 10.3390/sym12020253.

16. M.G. Murtaza, E.E. Tzirtzilakis, M. Ferdows, Numerical solution of three dimensional unsteady biomagnetic flow and heat transfer through stretching/shrinking sheet using temperature dependent magnetization, *Archives of Mechanics*, **70**(2): 161–185, 2018.

17. M. Ali, F. Ahmed, S. Hussain, Analytical solution of unsteady MHD blood flow and heat transfer through parallel plates when lower plate stretches exponentially, *Journal of Applied Environmental and Biological Sciences*, **5**(3): 1–8, 2015.

18. A. Zeeshan, A. Majed, R. Ellahi, Effect of magnetic dipole on viscous ferro-fluid past a stretching surface with thermal radiation, *Journal of Molecular Liquids*, **215**: 549–554, 2016.

19. I.H. Isaac Chen, Subrata Sana, Analysis of an intensive magnetic field on blood flow: Part 2, *Journal of Bioelectricity*, **4**(1): 55–62, 2009, doi: 10.3109/15368378509040360.

20. S. Srinivas, P.B.A. Reddy, B.S.R.V. Prasad, Effects of chemical reaction and thermal radiation on MHD flow over an inclined permeable stretching surface with non-uniform heat source/sink: An application to the dynamics of blood flow, *Journal of Mechanics in Medicine and Biology*, **14**(5): 1450067, 2014, doi: 10.1142/S0219519414500675.

21. A. Sinha, J.C. Misra, G.C. Shit, Effect of heat transfer on unsteady MHD flow of blood in a permeable vessel in the presence of non-uniform heat source, *Alexandria Engineering Journal*, **55**(3): 2023–2033, 2016, doi: 10.1016/j.aej.2016.07.010.

22. C. Israel-Cookey, A. Ogulu, V.B. Omubo-Pepple, Influence of viscous dissipation and radiation on unsteady MHD free-convection flow past an infinite heated vertical plate in a porous medium with time-dependent suction, *International Journal of Heat and Mass Transfer*, **46**(13): 2305–2311, 2003, doi: 10.1016/S0017-9310(02)00544-6.

23. E.M.A. Elbashbeshy, D.M.Yassmin, A.A. Dalia, Heat transfer over an unsteady porous stretching surface embedded in a porous medium with variable heat flux in the presence of heat source or sink, *African Journal of Mathematics and Computer Science Research*, **3**(5): 68–73, 2010, doi:10.5897/AJMCSR.9000071.

24. P.B.A. Reddy, N.B. Reddy, Radiation effects on MHD combined convection and mass transfer flow past a vertical porous plate embedded in a porous medium with heat generation, *International Journal of Applied Mathematics and Mechanics*, **6**(18): 33–49, 2010.

25. S. Nadeem, S. Zaheer, T. Fang, Effects of thermal radiation on the boundary layer flow of a Jeffery fluid over an exponentially stretching surface, *Numerical Algorithms*, **57**(2): 187–205, 2011, doi: 10.1007/s11075-010-9423-8.

26. P.B.A. Reddy, N.B. Reddy, S. Suneetha, Radiation effects on MHD flow past an exponentially accelerated isothermal vertical plate with uniform mass diffusion in the presence of heat source, *Journal of Applied Fluid Mechanics*, **5**(3): 119–126, 2012, doi: 10.36884/jatm.5.03.19454.

27. A.A. Khan, S. Muhammad, R. Ellahi, Q.M.Z. Zia, Bionic study of variable viscosity on MHD peristaltic flow of pseudoplastic fluid in an asymmetric channel, *Journal of Magnetics*, **21**(2): 273–280, 2016, doi: 10.4283/JMAG.2016.21.2.273.

28. P. Sreenivasulu, T. Poornima, N. Bhaskar Reddy, Thermal radiation effects on MHD boundary layer slip flow past a permeable exponential stretching sheet in the presence of joule heating and viscous dissipation, *Journal of Applied Fluid Mechanics*, **29**(1): 267–278, 2016.

29. F.T. Akyildiz, D.A. Siginer, K. Vajravelu, J.R. Cannon, R.A. Van Gorder, Similarity solutions of the boundary layer equations for a nonlinearly stretching sheet, *Mathematical Methods in the Applied Sciences*, **33**(5): 601–606, 2010, doi: 10.1002/mma.1181.

30. K. Bhattacharyya, G.C. Layek, R.S.R. Gorla, Boundary layer slip flow and heat transfer past a stretching sheet with temperature dependent viscosity, *Thermal Energy and Power Engineering*, **2**(1): 38–43, 2013.

31. A. Majeed, A. Zeeshan, F.M. Noori, U. Masud, Influence of rotating magnetic field on Maxwell saturated ferrofluid flow over a heated stretching sheet with heat generation/absorption, *Mechanics and Industry*, **20**(5): 502, 9 pp., 2019, doi: 10.1051/meca/2019022.

32. P. Ram, V. Kumar, Heat transfer in FHD boundary layer flow with temperature dependent viscosity over a rotating disk, *Fluid Dynamics and Materials Processing*, **10**(2): 179–196, 2014.

33. G. Bognár, K. Hriczó, Ferrofluid flow in magnetic field above stretching sheet with suction and injection, *Mathematical Modeling and Analysis*, **25**(3): 461–472, 2020, doi: 10.3846/mma.2020.10837.

34. A. Gizachew, B. Shanker, MHD flow of non-Newtonian viscoelastic fluid on stretching sheet with the effects of slip velocity, *International Journal of Engineer and Manufacturing Science*, **8**(1): 1–14, 2018.

35. A. Majeed, A. Zeeshan, R.S.R. Gorla, Convective heat transfer in a dusty ferromagnetic fluid over a stretching surface with prescribed surface temperature/heat flux including heat source/sink, *Journal of the National Science Foundation of Sri Lanka*, **46**(3): 399–409, 2018, doi: 10.4038/jnsfsr.v46i3.8492.

36. L.S.R. Titus, A. Abraham, Heat transfer in ferrofluid flow over a stretching sheet with radiation, *International Journal of Engineering Research and Technology*, **3**(6): 2198–2203, 2014.

37. L. Wahidunnsia, K. Subbarayudu, S. Suneetha, A novel technique for unsteady Newtonian fluid flow over a permeable plate with viscous dissipation, non-uniform heat source/sink and chemical reaction, *International Journal of Research in Engineering Application and Management*, **4**(10): 58–67, 2019.

38. S.R.R. Reddy, P.B.A. Reddy, S. Suneetha, Magnetohydrodynamic flow of blood in a permeable inclined stretching surface with viscous dissipation, non-uniform heat source/sink and chemical reaction, *Frontiers in Heat and Mass Transfer*, **10**(22), 10 pp., 2018, doi: 10.5098/hmt.10.22.

39. M.Q. Brewster, *Thermal Radiative Transfer and Properties*, John Wiley & Sons, New York, 1992.

40. E.E. Tzirtzilakis, A simple numerical methodology for BFD problems using stream function vortices formulation, *Communications in Numerical Methods in Engineering*, **24**(8): 683–700, 2008, doi: 10.1002/cnm.981.

41. H.I. Anderson, O.A. Valens, Flow of a heated ferrofluid over a stretching sheet in the presence of a magnetic dipole, *Acta Mechanica*, **128**: 39–47, 1998, doi: 10.1007/BF01463158.

42. E.E. Tzirtzilakis, M.A. Xenos, Biomagnetic fluid flow in a driven cavity, *Meccanica*, **48**(1): 187–200, 2013, doi: 10.1007/s11012-012-9593-7.

43. V.C. Loukopoulos, E.E. Tzirtzilakis, Biomagnetic channel flow in a spatially varying magnetic field, *International Journal of Engineering Sciences*, **42**: 571–590, 2014, doi: 10.1016/j.ijengsci.2003.07.007.

44. E. Magyari, B. Keller, Heat and mass transfer in the boundary layers on an exponentially stretching continuous surface, *Journal of Physics D: Applied Physics*, **32**(5): 577–585, 1999, doi: 10.1088/0022-3727/32/5/012.

45. M.A. El-Aziz, Viscous dissipation effect on mixed convection flow of a micropolar fluid over an exponentially stretching sheet, *Canadian Journal of Physics*, **87**(4): 359–368, 2009, doi: 10.1139/P09-047.

46. B. Bidin, R. Nazar, Numerical solution of the boundary layer flow over an exponentially stretching sheet with thermal radiation, *European Journal Scientific Research*, **33**(4): 710–717, 2009.

47. A. Ishak, MHD boundary layer flow due to an exponentially stretching sheet with radiation effect, *Sains Malaysiana*, **40**(4): 391–395, 2011.

Received March 1, 2021; revised version May 24, 2021.